Liquid Crystals

ISSN: (Print) (Online) Journal homepage: https://www.tandfonline.com/loi/tlct20

Multi-layered carbon nanotube UV polariser for photo-alignment of liquid crystals

Hoon Sub Shin , Ramesh Manda , Tae Hyung Kim , Jong Gil Park , Young Jin Lim , Byeong Koo Kim , Young Hee Lee & Seung Hee Lee

To cite this article: Hoon Sub Shin , Ramesh Manda , Tae Hyung Kim , Jong Gil Park , Young Jin Lim , Byeong Koo Kim , Young Hee Lee & Seung Hee Lee (2020) Multi-layered carbon nanotube UV polariser for photo-alignment of liquid crystals, Liquid Crystals, 47:11, 1604-1611, DOI: 10.1080/02678292.2020.1751318

To link to this article: https://doi.org/10.1080/02678292.2020.1751318

Published online: 22 Apr 2020.

LIQUID CRYSTALS
2020, VOL. 47, NO. 11, 1604–1611
https://doi.org/10.1080/02678292.2020.1751318

Taylor & Francis
Taylor & Francis Group

Check for updates

Multi-layered carbon nanotube UV polariser for photo-alignment of liquid crystals

Hoon Sub Shin[a,b], Ramesh Manda[a], Tae Hyung Kim[a], Jong Gil Park[c,d], Young Jin Lim[a], Byeong Koo Kim[b], Young Hee Lee[c,d*] and Seung Hee Lee[a*]

[a]Applied Materials Institute for BIN Convergence, Department of BIN Convergence Technology and Department of Polymer Nano Science and Technology, Jeonbuk National University, Jeonju, Korea; [b]LG Display Co., Ltd, Gumi, Gyungbuk, Korea; [c]Center for Integrated Nanostructure Physics(CINAP), Institute for Basic Science(IBS), Sungkyunkwan University, Suwon, Korea; [d]Department of Energy Science, Sungkyunkwan University, Suwon, Korea

ABSTRACT

An efficient ultraviolet (UV) polariser based on multi-layered carbon nanotubes (CNTs) which is obtained by set of CNT films attached to substrate in series with matching orientations is demonstrated. The degree of polarisation in the UV region increases with increasing number of CNT layers, reaching ~91% in the CNT polariser with 12 layers. A thin film with photoalignment polymer exposed with more than eight layers CNT polariser induces excellent homogenous liquid crystal (LC) alignment. The fringe-field switching (FFS) LC device with the photoalignment layer shows excellent electro-optics comparable to that with conventional metallic wire-grid polariser (WGP). The work proposes cost-effective novel polariser replacing WGP for photoalignment of LC.

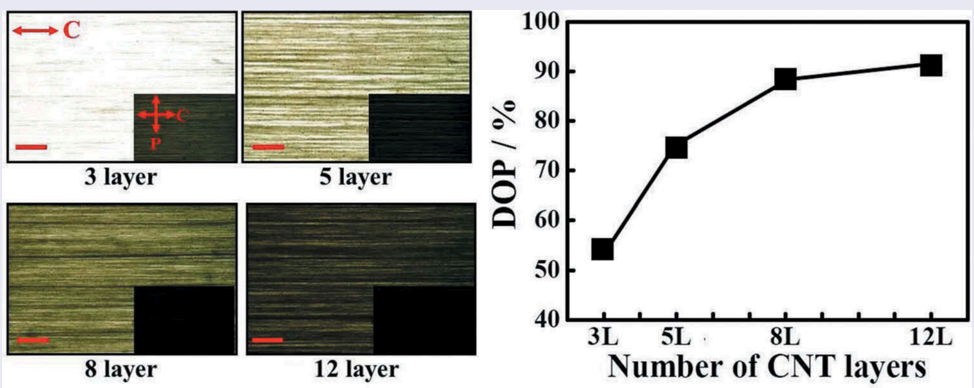

ARTICLE HISTORY
Received 3 February 2020
Accepted 31 March 2020

KEYWORDS
Carbon nanotubes; UV polariser; liquid crystal; fringe-field switching

Introduction

Liquid crystal displays (LCDs) are commercialised to all display applications such as television (TV), monitors, laptop personal computers, smart phones and automotive products because they exhibit good enough electro-optics performance with excellent reliability and a high image quality. More recently, competition between LCD and emissive organic light-emitting-diode (OLED) becomes fierce, forcing displays to show a better performance in both image quality and reliability. One of the major trends of displays is that the display resolution becomes higher and higher reaching 8 K in TV, over 500 ppi in mobile phones and over 1,000 ppi in virtual reality displays [1–6]. Among several LC devices, homogenously aligned FFS mode exhibits excellent electro-optic such as high transmittance, wide viewing angle, and low operating voltage, which is the reason many high-resolution LCDs adopt the mode [7]. The conventional way to achieve homogeneous alignment of LC is rubbing a polyimide-coated substrate with special velvet cloth. However, it creates rubbing-related issues such as nonuniform LC alignment and rubbing strengths, resulting in mura and light leakage in a dark state. That is the rubbing process deteriorates the image quality and contrast ratio of LCDs. Consequently, a non-rubbing photoalignment method that solves rubbing-related problems is started to adopt to improve the image quality of LCDs [8,9]. The polariser is essential for photoalignment. Although an efficient and polariser-free

CONTACT Seung Hee Lee lsh1@jbnu.ac.kr
*These authors contributed equally to this work.

photoalignment approach was proposed recently, the incident angle dependent pretilt angle formation is undesirable for FFS and IPS mode LCDs [10]. Therefore, utilisation of linearly polarised UV light is essential for photoalignment and the nano-WGP is generally used for this purpose [11]. However, WGP requires to have a very short pitch of about 100 nm to make UV light linearly polarised, which is highly cost process due to nanopattern of metals by either lift-off or reactive ion etching [12].

On other hand, the cheap conventional iodine polarisers are impossible to polarise UV light less than 380 nm due to strong UV absorption of iodine. One of the alternative methods to realise linearly polarised light is unidirectionally oriented carbon nanotube (CNT) bundles. The basic constituent of CNTs is graphite so that owing to the π plasmon-originated broad absorption spectrum and strong optical anisotropy of single-wall CNTs (SWCNTs), it shows a strong anisotropic optical activity in visible and ultraviolet (UV) wavelengths [13,14]. The polyvinyl alcohol (PVA) film in which SWCNTs are aligned along the stretching direction of the film exhibits 75–80% of degree of polarisation (DOP) in the region of 350–800 nm and moreover, the DOP and optical activity of SWCNT/PVA can be further improved by using shorter CNTs [14]. However, the efficiency of the CNT-based UV polariser is required to improve further to utilise in high image quality LCDs.

In this paper, the multi-layered CNT sheet, which acts as an efficient UV polariser, is demonstrated. The proposed multi-layered CNT polariser is showing high DOP of ~91% in UV region and is used as photomask for photo-aligning of reactive mesogen (RM)-doped polyimide (RM-PI) (Nissan Chemical Co., Japan) that provides efficient LC molecules alignment [15]. The fabricated FFS device [7] with photo-alignment of RM-PI through 12-layered CNT polariser exhibits comparable electro-optics to that made with WGP. The electro-optics of the device dependent on number of CNT layers in multi-layered CNT polarisers are studied in detail.

Experimental

Firstly, CNT forests are vertically grown on a silicon substrate by chemical vapour deposition technique [16–19] (A-tech system Co., Korea) in which each CNT yarn consists of ~15 nm width and ~350 μm long, as shown in Figure 1(a), and then a bundle of CNTs is stretched to make CNT sheet using mechanical rotation tool, in which the number of CNT layers is proportional to number of the rotation. The long axis of CNT layer in each sheet is parallel to the stretching direction in average, which is

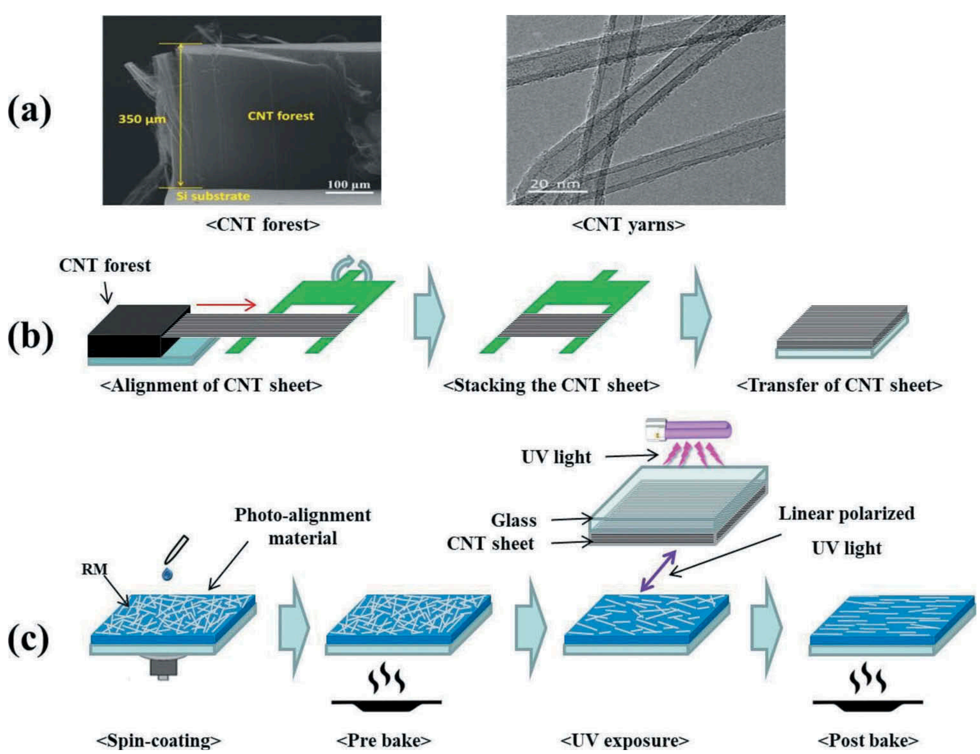

Figure 1. (Colour online) The schematic of experimental procedure for making anisotropic molecular arrangement in a photoalignment layer with CNT sheet: (a) SEM image of CNT forest and TEM image of CNT yarns; (b) CNT sheet is drawn from the grown CNT forest and then transferred to a glass substrate; and (b) Detailed process on how to get photo-alignment layer with anisotropy.

absorption axis of CNT polariser. Then the stacked CNT sheet is transferred to a glass substrate as indicated in Figure 1(b). The final multi-layered CNT polariser consists of 3, 5, 8 and 12 CNT sheets stacked together with matching orientations. The obtained multi-layered CNT polarisers has a potential to not only exhibit enough thermal stability but also possess high flexibility with capability to withstand mechanical damage due to bending. The obtained multi-layered CNT polariser is utilised for manipulating the alignment of nematic LC through photoalignment of RM-PI mixture which is a homogeneous mixture of photocurable RM solution dispersed in a thermally curable PI solution. The photoalignment layer of RM-PI was spin-coated with a thickness of 100 nm on an electrode-patterned glass substrate and then pre-baked at 80°C for 90 s to evaporate the solvent. The CNT sheet was positioned simply above the substrate and then 365 nm UV light (Hamamatsu Photonics K.K, Japan) was exposed with intensity of 5 mW/cm^2 for 15 s at room temperature, generating orientational ordering of polymerised mesogen in PI perpendicular to linearly polarised UV light like the same results reported already [15]. Finally, the layer was post-baked at 130°C for 10 min to improve the orientational ordering of mesogen in PI, as schematically shown in Figure 1(c). Here, we have employed FFS cell consisted of both patterned signal and plane common indium-tin-oxide (ITO) electrodes on bottom substrate while having no electrodes on the top substrate [7]. The signal electrode stripes are separated by 4.5 μm with uniform width of 3.5 μm. The signal and common electrodes are separated by very thin passivation with thickness of 0.5 μm. The dimension of substrate is 3 × 3 cm in length and width. Finally, two substrates are assembled one over another with cell gap of 3.4 μm and the LC infiltration was performed by capillary action at isotropic temperature of the LC. Here, a nematic LC with positive dielectric anisotropy of 4.7 and birefringence of 0.115 at 589 nm at 20°C (JNC Corp., Korea) is used. The CNT polariser with 3, 5, 8 and 12 CNT layers are used for controlling the polarisation state of the incident light.

At first, essential characterisations were performed with optical microscope and polarised optical microscope (POM) (Nikon eclipse, E600 POL) and UV–vis spectroscopy (Scinco, S-3100). The quality of the alignment is analysed with POM in detail and estimated by measuring the dark level from the off-state optical images by using an image analysing software i-solution^{TM} (iM Technology, i-Solution Inc.).

Results and discussion

Figure 2(a) shows optical microscopic images of prepared CNT polariser as a function of different CNT layers. Here, the inset images are obtained when the long axis of CNT axis is orthogonal to absorption axis of iodine-type polariser. The transmittance of the prepared polariser is compared with the traditional iodine based polariser (LG Chem., Korea) and WGP (Edmond optics, USA). One can easily notice that the relative transmittance of CNT polariser within visible region is

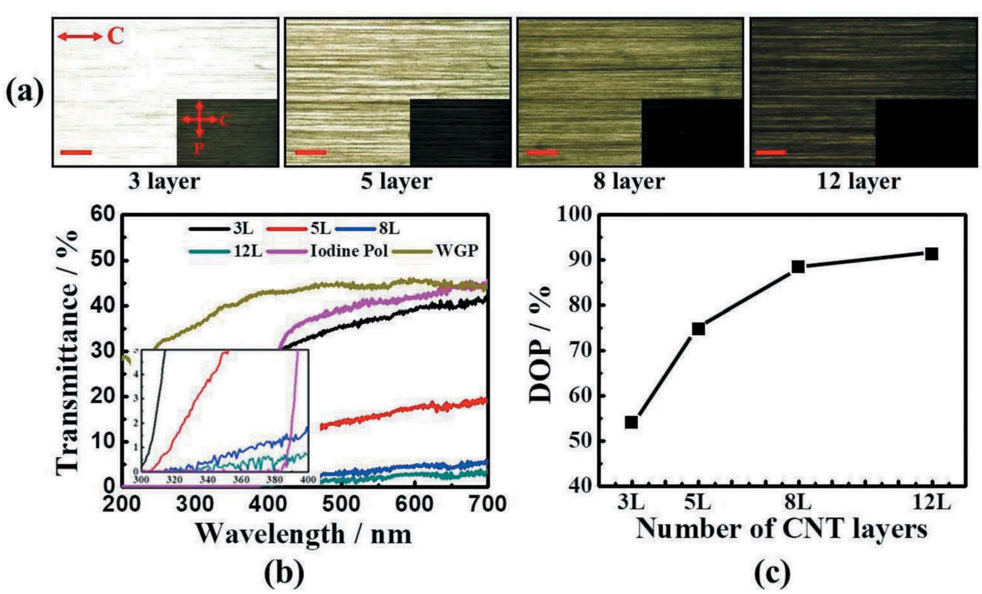

Figure 2. (Colour online) (a) Optical microscopic images of prepared multi-layered CNT polariser. C and P indicate a long axis of CNTs and iodine-type polariser, respectively. (Inset images are obtained when C and P are orthogonal to each other.) The scale bar indicates 100 μm. (b) Wavelength-dependent transmittances of each CNT sheet and iodine polariser. (c) Calculated DOP of CNT sheet as a function of number of CNT layers at 365 nm.

decreasing with increasing number of CNT layers. Further, the density of dark lines along the CNT stretching direction, which comes from a complete absorption of light parallel to the CNT rods, is increasing with number of CNT layers. These findings indicate that the incident light with its electric vector parallel (perpendicular) to the stretched CNT axis is effectively absorbed (transmitted) by the multi-layered CNT polarisers. Wavelength-dependent transmittance is showing a good correlation with optical microscopic results, as shown in Figure 2(b). The transmittance of CNT polariser at 365 nm is measured to be >10%, 6.5%, 1.0% and 0.5% for 3, 5, 8 and 12 CNT layers, respectively, whereas the iodine polariser is exhibiting almost zero transmittance. Moreover, the proposed CNT polariser is capable to extend the absorption of incident light up to deep UV region providing a wider operating wavelength range from 300 nm to 400 nm and all multi-layered CNT polarisers exhibit high stability against long time UV exposure. Further, we measure a DOP that indicates its polarising capability, defined as,

$$\mathrm{DOP} = \sqrt{\frac{T_{//} - T_{\perp}}{T_{//} + T_{\perp}}} \times 100 \qquad (1)$$

where $T_{//}$ and $T_{\perp}$ are transmittances of the CNT polariser when it is aligned parallel and perpendicular to the plane of polarisation of incident light through WGP, respectively. Interestingly, the DOP is monotonically increasing from 54.1% to 91.3%, at 365 nm, by increasing the number of CNT layers from 3 to 12, as shown Figure 2(c). This observation implies that the CNT sheet with densely packed CNT layers in series with matching orientations effectively attenuates the incident light in parallel to the CNT bundles while allowing the light in perpendicular to the CNT bundles, giving rise to good polarised light at 365 nm.

In order to investigate feasibility to replace conventional WGP with proposed device, the multi-layered CNT polarisers are further utilised for photoalignment of RM-PI mixture and subsequent observation are performed under the POM. In first case, the nonpolarized UV irradiation was performed directly to the substrate. In second case, the irradiation of UV was performed to the CNT polariser positioned above the substrate with alignment layer. The sample was then thermally cured to polymerise the PI in the RM-PI mixture. The POM images in Figure 3(a,b) exhibit a complete dark state irrespective of the substrate direction, indicating no preferred orientation of polymerised mesogen in the layer. However, POM images in Figure 3(c,d) clearly exhibit extinction and bright state when the polarising direction of five layered CNT polariser is coincident and makes 45° with crossed polarisers, respectively, indicating an orientational ordering of polymerised mesogen is achieved. Conclusively speaking, the photoalignment layer becomes optically anisotropic after UV exposure through multi-layered CNT sheet, that is, the CNT sheet produces the linear polarised state in a UV region enough to induce anisotropic orientation of mesogen.

Next, we measured a polarisation state of the transmitted UV light by rotating two 5 layer CNT polariser.

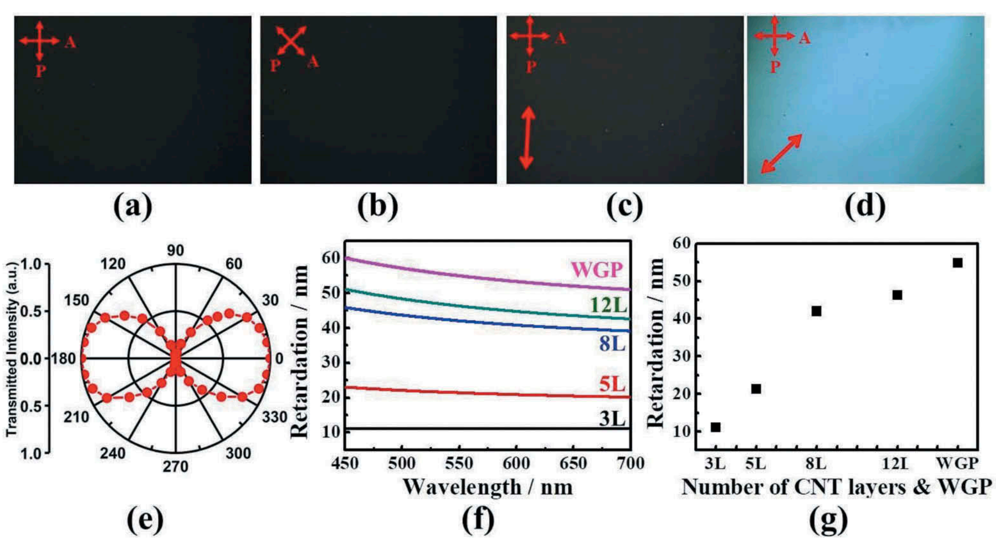

Figure 3. (Colour online) POM images of RM-PI layers polymerised without CNT film (a) and (b), and with CNT film (c) and (d). Under exposure of nonpolarized UV, no birefringence in photoalignment layer is induced [(a) and (b)] while the birefringence coming from orientational ordering of mesogen in the layer is clearly induced (c) and (d). P and A represent the polariser and analyser of POM and the arrow indicates a polarising direction of CNT polariser with 5 layers. (e) Measured polarisation state of transmitted light. Measured wavelength-dependent retardation (f) and retardation at 550 nm (g) of photoalignment layer with conventional WGP and CNT sheets consisted of 3, 5, 8 and 12 layers.

As seen in Figure 3(e), the maximum transmission was found when two multi-layered CNT polarisers are parallel to each other, while the transmitted intensity was found to be zero when those are crossed (90°). The polarisation axis of the transmitted UV light is perpendicular to stretching direction of the CNT polariser. These results are direct evidence of emission of linearly polarised light from multi-layered CNT polariser in UV regime.

In order to see more insights, we have further measured retardation of the photoaligned RM-PI layer in a wavelength range from 450 nm to 720 nm. The obtained retardation is 11 nm, 21 nm, 42 nm and 46 nm for a CNT polariser with 3, 5, 8 and 12 layers, whereas the conventional WGP shows 55 nm, respectively, as shown in Figure 3(f,g). Evidently, the retardation tends to increase with increasing number of CNT layers, which makes sense because the DOP follows the same trend. Higher retardation means more anisotropic surface is achieved, which can offer a better anchoring strength for LC. However, the retardation achieved by conventional WGP is 55 nm at 550 nm, which is slightly larger than that of the 12-layer CNT polariser.

Motivated by these results, we have prepared FFS-LC cells and investigated their electro-optics while applying a square-wave voltage with 1 kHz. Here, initial LC orientation is set to 7° with respect to the signal electrode direction. At first, we check the black state of the sample exposed with a linearly polarised UV light by using the multi-layered CNT polariser. For qualitative results, these results are compared with the condition where no multi-layered CNT polariser was utilised. As illustrated in Figure 4(a–d), the samples those UV cured with CNT polariser exhibit a dark state under crossed polarisers because the long axis of LC is arranged perpendicular to the incident polariser, that is, parallel to the CNT orientation. In contrary, the sample which is UV cured without CNT polariser is not showing any dark state because the LC is randomly aligned as shown in Figure 4(e). Very interestingly, all FFS cells show a good dark state irrespective of number of CNT layers in the CNT polariser, as clearly shown in POM images of Figure 5(a–d). In order to evaluate quality of the dark level more details, the POM images were analysed by an image analysing software i-solution™ (iM Technology, i-Solution Inc.). The measured dark levels are 1.60, 1.38, 1.34 and 1.31 for 3, 5, 8 and 12 CNT layers, respectively, indicating a better orientational ordering of LC along one direction is achieved in higher number of CNT layers.

Nevertheless, POM images at field-on state shows a distinct behaviour between cells. For instance, the FFS cells exposed with 3 and 5 CNT layers are exhibiting slight nonuniformity in brightness of low grey scales called mura at 3 V (see magnified image in Figure 5(e)), whereas the cells exposed with 8 and 12 CNT layers do not show such mura (see magnified image in Figure 5(f)). This nonuniformity observed in field on state can be observed only in the case the azimuthal anchoring strength is not uniform enough because it comes from difference in the rotating degree of LC at 3 V. Further, there is no noticeable transmittance difference at high grey bright state (7 V), since the dielectric coupling dominates over other LC–LC and LC-interface related forces. We infer that the mura at 3 V is associated with low DOP of the CNT polariser because the lower the DOP the orientation of the CNT deviates more from mean orientation or the absorption level of UV along the CNT stretching direction is lower, as proven by nonuniform dark lines in Figure 2(a). In other words, the orientation ordering of RM induced by CNT sheet is not uniform enough from position to position, giving rise to

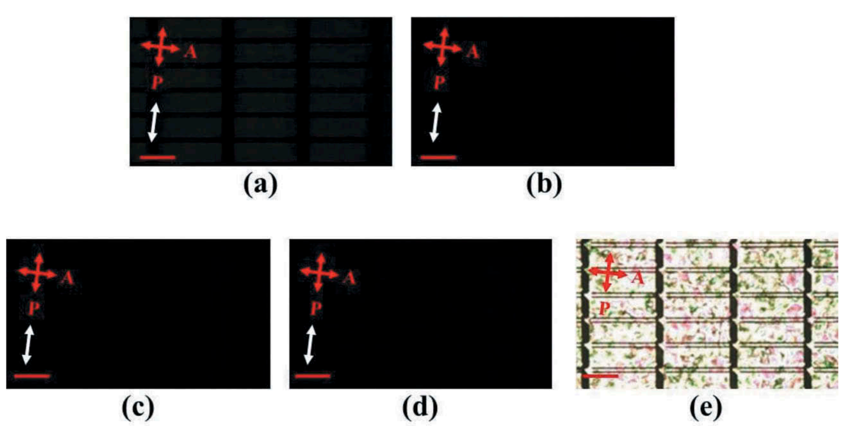

Figure 4. (Colour online) Off-state POM images of the fabricated FFS cells under crossed polarisers after UV exposure with CNT sheets with different number of CNT layers: (a) 3, (b) 5, (c) 8, (d) 12 and (e) no CNT sheet. P and A represent the polariser and analyser of POM and the arrow indicates a long axis of liquid crystal. The scale bar indicates 100 μm.

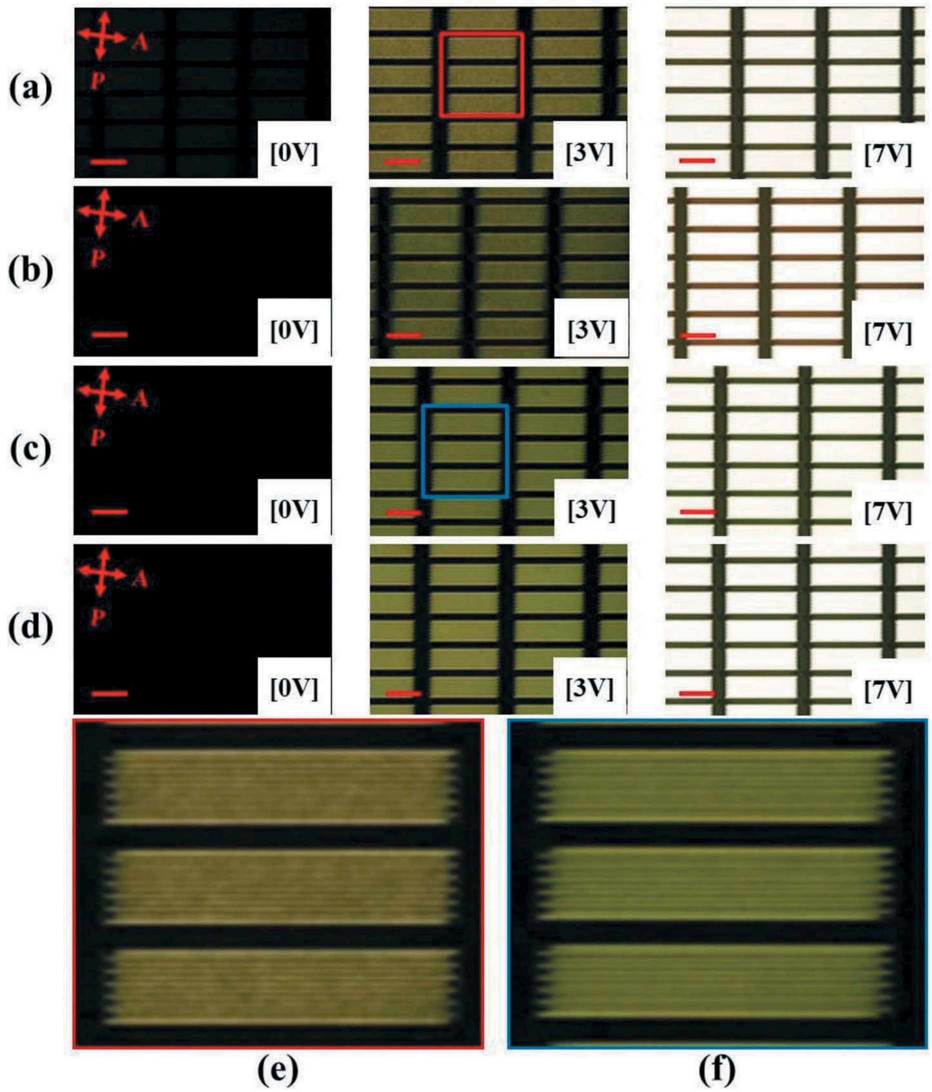

Figure 5. (Colour online) POM images while increasing voltages from dark to white states in UV-aligned FFS cells with CNT sheets having different number of CNT layers: (a) 3, (b) 5, (c) 8 (d) 12, and magnified one-pixel images at 3 V in a red (e) and blue (f) box. The scale bar indicates 100 μm.

nonuniform azimuthal anchoring strength, as schematically shown in Figure 6. Therefore, we expect the UV exposure with low DOP CNT polariser not only gives rise to less orientational ordering in the initial optic axis but also its anchoring strength is not uniform enough, dividing exposed regions into weak and strong anchoring. However, the DOP more than 85% for 8 and 12-layered CNT polarisers is good enough to induce both uniform optics axis and anchoring strength of LC, as shown in Figure 6.

At the final step, the response time of the FFS cell is measured as a function of CNT layers. The rising time (τ_{on}) and falling time (τ_{off}) are defined as the time required for changing the transmittance from 10% to 90% and 90% to 10%, respectively. The falling time (τ_{off}) is mainly associated with elastic relaxation of LC molecules back to original position upon voltage withdrawn. The τ_{on} and τ_{off} times are derived from dielectric response and director relaxation dynamics, which is expressed as [20],

$$\tau_{on} = \frac{\gamma_1}{\varepsilon_0|\Delta\varepsilon|E^2 - \frac{\pi^2}{d^2}K_{22}} = \frac{\gamma_1}{\varepsilon_0|\Delta\varepsilon|E^2 - 2\frac{W}{d}} \quad (2)$$

$$\tau_{off} = \frac{\gamma_1 d^2}{K_{22}\pi^2} = \frac{\gamma_1 d}{2W} \quad (3)$$

where, γ_1 is a rotational viscosity, K_{22} is a twist elastic constant, E is an electric field strength, d is a cell gap, $\Delta\varepsilon$ is a dielectric anisotropy of LC and W is a surface anchoring energy of LC molecules with alignment layer. As we understand from the Equation (2) and

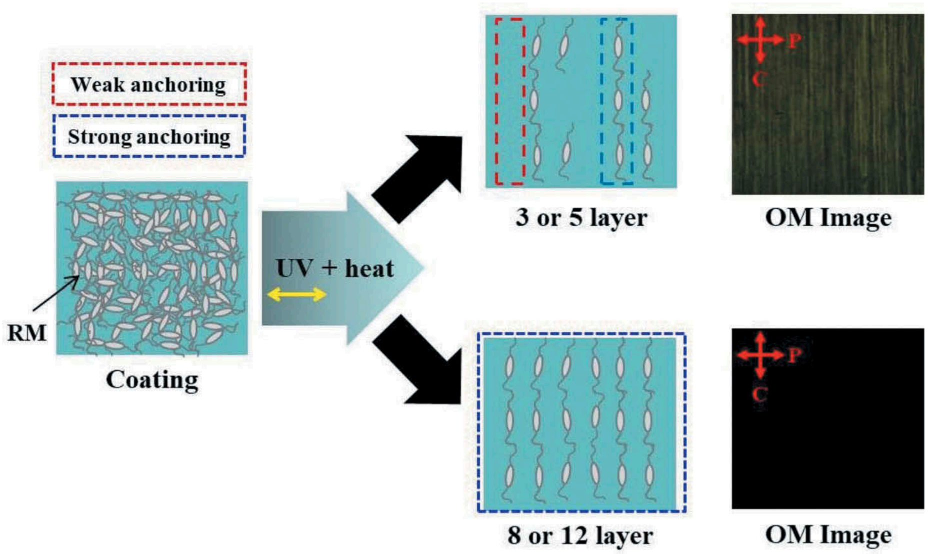

Figure 6. (Colour online) The schematic of anchoring mechanism of LC molecules on RM-PI surface exposed with CNT sheet having different number of CNT layers.

(3), the alteration in both τ_{on} and τ_{off} originates from difference in anchoring strength of LC at photoalignment layer since the same LC is used for all the cells.

It has been well known weak anchoring energy between LC and alignment layer leads to shorter τ_{on} and longer τ_{off}, compared with strong anchoring energy [20,21]. The τ_{on} and τ_{off} of WGP sample are measured to be 7.5 ms and 12.8 ms, respectively. Interestingly, τ_{off} of the FFS cell decreases with increasing CNT layers such that it is 28.8 ms for 3 layers but 13.1 ms for 12 layers of CNT, whereas the τ_{on} is mostly unaltered, as shown in the Figure 7. Since the same LC is employed in all the cells, the anchoring strength of the sample could be the reason for changes in τ_{off}, as theoretically interpreted with Equation (3). The retardation of the RM-PI increases with increasing CNT layers as shown in Figure 4(f), and so does W. In addition, the highest retardation is achieved from use of WGP so that we expect W is larger than those of CNT polariser. Consequently, τ_{off} becomes shorter with increasing CNT layers and exhibits comparable value to that of WGP when the 12-layered CNT polariser is used, which well correlates with our qualitative analysis.

Overall, the photoaligned FFS cell utilising CNT polariser exhibits comparable electro-optics to those of WGP, which reveals a potential to replace conventional WGP with high-cost and nano-patterning. In addition, the obtained multi-layered CNT polarisers has a potential to not only exhibit enough thermal stability because the CNT is stable over 400° C in air [22] but also possess high flexibility capable of withstanding mechanical damage due to bending.

Finally, we are working on improving the DOP of CNT polariser by controlling density of grown CNT forests by chemical vapour deposition and stretching method because higher DOP gives rise to higher induced retardation in the applied photoalignment layer, which results in better LC alignment and fast falling time.

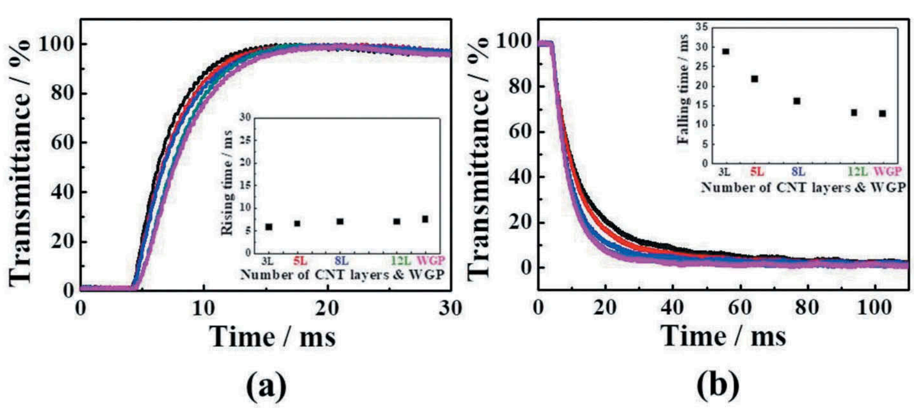

Figure 7. (Colour online) Rising (τ_{on}) and falling (τ_{off}) response times of the FFS cell depending on number of CNT layers in the CNT sheets.

Conclusion

We propose a multi-layered CNT based UV polariser which exhibits higher DOP of 91% by matching orientation of stacked CNTs in each layer. A novel approach for LC alignment is demonstrated through photoalignment of RM-PI by utilising multi-layered CNT polariser that can be utilised for FFS-LCD. Although, the RM-PI layer photoaligned through 3-layered CNT polariser exhibits imperfect dark state, a low grey mura and relatively slow falling response time, a CNT polariser with more layers, for instance, 8 and 12-layered CNT polarisers, exhibit excellent uniformity in LC alignment and electro-optics. Especially, 8-layered CNT polariser is of great importance for practical applications, as it exhibits high transmittance, high DOP, and fast response time. For the first time to our knowledge, we propose the multi-layered CNT polariser applying for photoalignment layer of LC, which can replace the WGPs. We believe it has strong potentiality to utilise in future photonic and electro-optic devices with broadband gap from UV to infrared.

Disclosure statement

The authors declare no competing financial interest.

Funding

This research was supported by the Basic Science Research Program through the National Research Foundation of Korea (NRF) funded by the Ministry of Education (2016R1D1A1B01007189) and the Korea Government (MSIT) funded through the National Research Foundation of Korea (NRF) (No. 2019R1A5A8080326).

ORCID

Ramesh Manda http://orcid.org/0000-0002-6171-7991

References

[1] Jung YK, Choi HS, Ahn SY, et al. 3 stacked top emitting white OLED for high resolution OLED TV. SID Int Symp Dig Tech Pap. 2016;47:707–710.
[2] Nakata M, Motomura G, Nakajima Y, et al. Development of flexible displays using back-channel-etched In-Sn-Zn-O TFTs and air-stable inverted OLEDs. SID Int Symp Dig Tech Pap. 2015;46:969–972.
[3] Bae KS, Oh M, Park B, et al. Novel pixel structure for 8K QUHD LCD panel with the enhanced optical performances. SID Int Symp Dig Tech Pap. 2019;50:703–706.
[4] Ono K, Hiyama I. The latest IPS pixel structure suitable for high resolution LCDs. Proceedings of the 19th International Display Workshops in Conjunction with Asia Display (Society for Information Display); Dec 4–7; Kyoto (Japan); 2012. p. 933–936.
[5] Ono K, Matsukawa H. High performance IPS technology suitable for high resolution LCDs. Proceedings of the 20th International Display Workshops (Society for Information Display); Dec 4–6; Sapporo, Japan; 2013. p. 24–25.
[6] Yoon JH, Lee SJ, Lim YJ, et al. Fast switching, high contrast and high resolution liquid crystal device for virtual reality display. Opt Express. 2018;26:34142–34149.
[7] Lee SH, Lee SM, Kim HY, et al. Ultra-FFS TFT-LCD with super image quality and fast response time. SID Int Symp Dig Tech Pap. 2001;32:484–487.
[8] Gelbaor M, Klebanov M, Lyubin V, et al. Photoinduced permanent alignment of liquid crystal on nanostructured chalcogenide thin film. Appl Phys Lett. 2011;98:071909.
[9] Zhong ZX, Li X, Lee SH, et al. Liquid crystal photoalignment material based on chloromethylated polyimide. Appl Phys Lett. 2004;85:2520–2522.
[10] Chigrinov VG, Kozenkov VM, Kwok HS. Photoalignment of liquid crystalline materials: physics and applications. New York: John Wiley & Sons; 2008.
[11] Hu W, Srivastava A, Xu F, et al. Liquid crystal gratings based on alternate TN and PA photoalignment. Opt Express. 2012;20:5384–5391.
[12] Ling J, Wang X, Liu X, et al. Tunable structure of nanowire-grid polarizer for deep ultraviolet region. Optik. 2018;158:1543–1547.
[13] Kataura H, Kumazawa Y, Maniwa Y, et al. Optical properties of single-wall carbon nanotubes. Synth Met. 1999;103:2555–2558.
[14] Shoji S, Suzuki H, ProiettiZaccaria R, et al. Optical polarizer make of uniaxially aligned short single-wall carbon nanotubes embedded in a polymer film. Phys Rev. 2008;B77:153407.
[15] Goto K, Yamanouchi H, Ashizawa R, et al. Novel photoaligment layer for in plane switching mode LCD using 313nm ultraviolet light. SID Int Symp Dig Tech Pap. 2013;44:537–540.
[16] Merkulov V, Melechko A, Guillorn M, et al. Alignment mechanism of carbon nanofibers produced by plasma-enhanced chemical-vapor deposition. Appl Phys Lett. 2001;79:2970–2972.
[17] Jo SH, Tu Y, Huang ZP, et al. Effect of length and spacing of vertically aligned carbon nanotubes on field emission properties. Appl Phys Lett. 2003;82:3520–3522.
[18] Hooijdonk EV, Bittencourt C, Snyders R, et al. Functionalization of vertically aligned carbon nanotubes. Beilstein J Nanotechnol. 2013;4:129–152.
[19] Choi YC, Shin YM, Lee YH, et al. Controlling the diameter growth rate, and density of vertically aligned carbon nanotubes synthesized by microwave plasma-enhanced chemical vapor deposition. Appl Phys Lett. 2000;76:2367–2369.
[20] Nie X, Lu R, Xianyu H, et al. Wu, Anchoring energy and cell gap effects on liquid crystal response time. J Appl Phys. 2007;101:103110.
[21] Nehring J, Kmetz AR, Scheffer TJ. Analysis of weak-boundary-coupling effects in liquid-crystal displays. J Appl Phys. 1976;47:850–857.
[22] Mahajan A, Kingon A, Kukovecz A, et al. Studies on the thermal decomposition of multiwall carbon nanotubes under different atmospheres. Mater Lett. 2013;90:165–168.